Metabolic engineering optimizes bioorthogonal glycan labeling in living cells

Anna Cioce[a,b,¶], Ganka Bineva-Todd[b,¶], Anthony J. Agbay[c], Junwon Choi[c,£], Thomas M. Wood[c,$], Marjoke F. Debets[c,#], William M. Browne[a,b], Holly L. Douglas[d], Chloe Roustan[e], Omur Y. Tastan[b], Svend Kjaer[e], Jacob T. Bush[f], Carolyn R. Bertozzi[c,g], Benjamin Schumann[a,b,*]

[a]Department of Chemistry, Imperial College London, 80 Wood Lane, W12 0BZ, London, United Kingdom.

[b]The Chemical Glycobiology Laboratory, The Francis Crick Institute, 1 Midland Rd, NW1 1AT London, United Kingdom.

[c]Department of Chemistry, Stanford University, Stanford, CA 94305, USA.

[d]Mycobacterial Metabolism and Antibiotic Research Laboratory, The Francis Crick Institute, 1 Midland Rd, NW1 1AT London, United Kingdom.

[e]Structural Biology Science Technology Platform, The Francis Crick Institute, NW1 1AT London, United Kingdom.

[f]GlaxoSmithKline, Gunnels Wood Road, Stevenage, Hertfordshire, SG1 2NY UK.

[g]Howard Hughes Medical Institute, 380 Roth Way, Stanford, CA 94305, USA.

[£]Current address: Department of Molecular Science and Technology, Ajou University, Suwon 16499, Republic of Korea.

[$]Current address: Biological Chemistry Group, Institute of Biology Leiden, Leiden University, Sylvius Laboratories, Sylviusweg 72, 2333 BE Leiden, The Netherlands.

[#]Current address: Lilly Research Laboratories, Eli Lilly and Company, Indianapolis, IN 46285, USA.

[¶]These authors contributed equally.

*Correspondence should be addressed to: b.schumann@imperial.ac.uk.

Abstract

Metabolic oligosaccharide engineering (MOE) has fundamentally contributed to our understanding of protein glycosylation. Efficient MOE reagents are activated into nucleotide-sugars by cellular biosynthetic machineries, introduced into glycoproteins and traceable by bioorthogonal chemistry. Despite their widespread use, the metabolic fate of many MOE reagents is only beginning to be mapped. While metabolic interconnectivity can affect probe specificity, poor uptake by biosynthetic salvage pathways may impact probe sensitivity and trigger side reactions. Here, we use metabolic engineering to turn the weak alkyne-tagged MOE reagents Ac_4GalNAlk and Ac_4GlcNAlk into efficient chemical tools to probe protein glycosylation. We find that bypassing a metabolic bottleneck with an engineered version of the pyrophosphorylase AGX1 boosts nucleotide-sugar biosynthesis and increases bioorthogonal cell surface labeling by up to two orders of magnitude. Comparison with known azide-tagged MOE reagents reveals major differences in glycoprotein labeling, substantially expanding the toolbox of chemical glycobiology.

Introduction

Protein glycosylation is an important modulator of biological processes. Chemical MOE reagents have developed into important alternatives to protein-based binding reagents to profile the roles of glycans in cellular processes.[1–4] Monosaccharides with chemical modifications can be fed to living cells as caged analogs, are metabolically activated and introduced into the glycome by the activity of glycosyltransferases (GTs).[1,4–6] Modifications such as azides or alkynes can be probed by bioorthogonal ligation using Cu(I)-assisted azide-alkyne cycloaddition (CuAAC) to allow for visualization and characterization of glycoconjugates.[2,4,7,8] While it is generally accepted that small chemical perturbations are compatible with metabolic activation, the actual fate and turnover efficiency of modified monosaccharides is only beginning to be understood. Key to use by GTs is the biosynthesis of modified nucleotide-sugars, such as derivatives of uracil diphosphate (UDP)-activated *N*-acetylgalactosamine (GalNAc) and *N*-acetylglucosamine (GlcNAc) (Fig. 1A). The salvage pathway of GalNAc derivatives

features the kinase GALK2 and the pyrophosphorylases AGX1/2, while GlcNAc derivatives have to be activated by the kinase NAGK, the mutase AGM as well as AGX1/2.[9,10] In the cytosol of mammalian cells, derivatives of UDP-GalNAc and UDP-GlcNAc can be interconverted by the UDP-GalNAc/GlcNAc 4'-epimerase GALE, which interconnects both nucleotide-sugar pools. Epimerization substantially decreases the glycan specificity while enhancing the labeling efficiency of certain MOE reagents and can be suppressed by careful choice of the chemical modification.[10–12] Once biosynthesized, derivatives of UDP-GalNAc and UDP-GlcNAc can be used as substrates by cellular GTs, including the large polypeptide GalNAc transferase (GalNAc-T) family in the secretory pathway and a myriad of GlcNAc transferases in several cellular compartments.

Recent years have seen increasing evaluation of the metabolic fate of MOE reagents. Although the enzymes of GalNAc and GlcNAc salvage pathways generally display reduced efficiency towards modifications on the acetamide side chain, the relatively small azide group is accepted as part of reliable MOE reagents.[10,12–15] In contrast, large modifications prevent enzymatic activation of GalNAc and GlcNAc analogs.[11,16,17] Yu et al. thus developed an engineered version of AGX1 (mutant F383G) to increase substrate promiscuity and biosynthesize UDP-GlcNAc analogs from the corresponding GlcNAc-1-phosphate analogs that can be delivered through caged precursors.[16] We have used the similar F383A mutant, herein termed mut-AGX1, to biosynthesize UDP-GalNAc analogs that would normally not be made in the living cell.[4,11,17] Somewhat surprisingly and contrary to azide-tagged analogs of similar size, Batt et al. found that the most simple alkyne-tagged UDP-GalNAc and UDP-GlcNAc derivatives, UDP-GalNAlk **1** and UDP-GlcNAlk **2**, are biosynthesized in varying and often low efficiency in mammalian cells (Fig. 1A).[18] Metabolic incompatibility thus impairs the efficiency of precursors of **1** and **2**, Ac_4GalNAlk and Ac_4GlcNAlk, as MOE reagents despite their straightforward commercial access and potential GT acceptance.[19]

Here, we profile the metabolic fate of the weak MOE reagents Ac_4GalNAlk and Ac_4GlcNAlk in order to turn both reagents into highly efficient tools to probe cell surface glycosylation. We find that mut-AGX1

effectively biosynthesizes UDP-GalNAlk **1** and UDP-GlcNAlk **2** with greatly increased efficiency over WT-AGX1 from caged precursors that can thus be used to profile cell surface protein glycosylation. By suppressing GALE-mediated epimerization, we further find that UDP-GalNAlk **1** and UDP-GlcNAlk **2** enter different subsets to azide-tagged analogs, potentially due to differential acceptance by GTs. We show that close monitoring of the biosynthetic fate enables the development of highly effective MOE reagents.

Results and Discussion

To study the metabolic fate of UDP-GAlNAlk **1** and UDP-GlcNAlk **2**, we first assessed *in vitro* whether both reagents are epimerized by GALE (Fig. 1B). Incubation of synthetic **1** with either a wild type (WT), GALE-containing cell lysate or purified GALE led to epimerization to **2**, as detected either by ion-pair HPLC or high performance anion exchange chromatography (HPAEC). A lysate made from GALE-KO cells did not lead to epimerization. We next profiled the suitability of UDP-GalNAlk **1** as a substrate for members of the GalNAc-T family. GalNAc-Ts prime highly abundant mucin-type protein O-GalNAc glycans, and acceptance of **1** would thus correlate with high cell surface labeling efficiency. Synthetic peptides served as acceptor substrates in *in vitro* glycosylation experiments. Compared to the native substrate UDP-GalNAc, UDP-GalNAlk **1** was used with lower but well-measurable efficiency by GalNAc-T1 and T2, and similar efficiency by GalNAc-T7 and T10 (Fig. 1C). The isoenzymes T7 and T10 differ from T1 and T2 in their preference of pre-O-GalNAc-glycosylated substrate peptides, which may hint to the use of UDP-GalNAlk **1** as a GalNAc-T subset-selective substrate.[20]

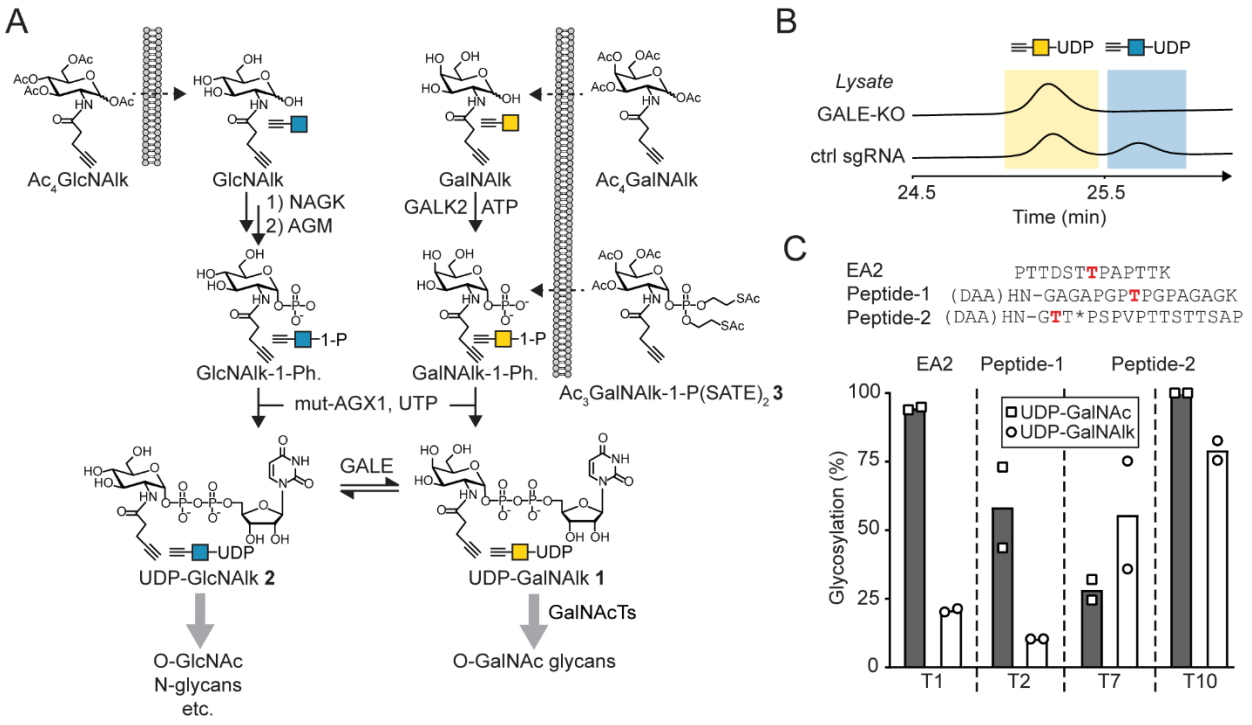

93

94 **Fig. 1:** The metabolic fate of GalNAlk and GlcNAlk. *A*, biosynthesis of UDP-GalNAlk **1** and UDP-
95 GlcNAlk **2** from caged precursors using salvage pathways. Dashed arrows indicate diffusion across
96 membranes and (thio-esterases). *B*, *in vitro* epimerization of UDP-GalNAlk **1** (yellow) to UDP-GlcNAlk
97 **2** (blue) using a GALE-containing cell lysate, or a GALE-KO lysate as a control as assessed by HPAEC.
98 The reaction was also performed using purified GALE, and retention times were compared to standards
99 (Fig. S1). *C*, *in vitro* glycosylation with purified GalNAc-Ts of synthetic peptides using UDP-GalNAlk **1**
100 or UDP-GalNAc as substrates. Red amino acids are new glycosylation sites. T* denotes α-D-GalNAc-Thr
101 Data are individual measurements of biological duplicates and means. The reactions using UDP-GalNAc
102 as a substrate have been used previously.[11]

103

104 We next studied the biosynthesis of UDP-GalNAlk **1** and UDP-GlcNAlk **2** in cells fed with caged,
105 membrane-permeable precursors. Since AGX1 has been identified as a metabolic bottleneck of other
106 modified GalNAc analogs, we synthesized caged GalNAlk-1-phosphate **3** to specifically probe AGX1-

mediated biosynthesis of UDP-GalNAlk **1**.[4,11,17] We tested UDP-sugar biosynthesis from **3** in K-562 cells with either normal GALE expression or a GALE-knockout and stably transfected with either mut-AGX1, WT-AGX1 or empty vector. HPAEC revealed measurable biosynthesis of both UDP-GalNAlk and UDP-GlcNAlk in the presence of mut-AGX1, but not WT-AGX1 (Fig. 2A). Free GalNAlk-1-phosphate was detectable in all cases, as observed by comparison with a synthetic standard (Fig. 2A). In the absence of GALE, UDP-GlcNAlk was not detectable, indicating that UDP-GalNAlk is biosynthesized by mut-AGX1 and subsequently epimerized by GALE in the cytosol.

We then assessed metabolic cell surface labeling mediated by caged GalNAlk-1-phosphate **3** by flow cytometry. The clickable fluorophore AF488-picolyl azide was used in non-cytotoxic Cu(I)-click CuAAC conditions to visualize labeling.[8,21] The presence of mut-AGX1 led to a dose-dependent increase of fluorescence by up to two orders of magnitude compared to WT-AGX1 (Fig. 2B). Of note, the presence of WT-AGX1 still led to discernible cell surface labeling, indicating that UDP-GalNAlk can be biosynthesized at levels that are too low to detect chromatographically. This was especially pronounced in GALE-KO cells in which no endogenous UDP-GalNAc is present to compete with UDP-GalNAlk **1** as substrates of GalNAc-Ts (Fig. 2B, Fig. S2B). A labeling difference of one order of magnitude was observed between cells expressing WT-AGX1 and mut-AGX1 when fed with Ac_4GlcNAlk, indicating that mut-AGX1 also mediates UDP-GlcNAlk **2** biosynthesis (Fig. S2A). Increasing UDP-GalNAc levels in these cells by supplementing cell culture media with free GalNAc led to a decrease of UDP-GalNAlk **1**-dependent labeling signal (Fig. 2C, Fig. S2C).[17] Likewise, labeling signal by Ac_4GlcNAlk was abrogated by addition of free GlcNAc (Fig. 2C). In contrast, labeling by the control compound Ac_4ManNAlk, an MOE reagent that enters the biosynthetic pathway of the sugar sialic acid, was unchanged irrespective of AGX1 overexpression or addition of free GalNAc or GlcNAc (Fig. 2C, Fig. S2B). Enhancing the levels of native UDP-sugars thus competed out incorporation of GalNAlk and GlcNAlk, but not ManNAlk, into glycoproteins. We concluded that AGX1 is likely a bottleneck in the biosynthesis of both UDP-GalNAlk **1** and UDP-GlcNAlk **2**, impairing metabolic labeling which can be

enhanced by stable overexpression of mut-AGX1, but not WT-AGX1. Our data further indicate that Ac_4GalNAlk exhibits low-level metabolic glycoprotein labeling without mut-AGX1 expression in line with findings of Zaro et al.[7] UDP-GalNAlk **1** formation is not measurable under these conditions, underlining the highly inefficient biosynthesis of **1** by the GalNAc salvage pathway without mut-AGX1.[18]

As overexpression of mut-AGX1 enabled cell surface labeling from Ac_4GlcNAlk, GlcNAlk-1-phosphate biosynthesis from the free monosaccharide by NAGK/AGM1 was apparently not a major metabolic bottleneck. We next assessed whether UDP-GalNAlk **1** biosynthesis followed the same principles which would, in turn, allow us to use the readily available MOE reagent Ac_4GalNAlk instead of caged GalNAlk-1-phosphate **3**. We found that mut-AGX1, but not WT-AGX1, efficiently biosynthesized UDP-GalNAlk **1** and UDP-GlcNAlk **2** from the per-acetylated precursors Ac_4GalNAlk and Ac_4GlcNAlk, respectively, in living cells (Fig. S3). We note that the 'upstream' precursors Ac_4GalNAlk and Ac_4GlcNAlk required longer feeding times (12-16 hours instead of 6-9 hours) than caged GalNAlk-1-phosphate **3** until UDP-sugar biosynthesis could be detected, in line with additional enzymatic reactions being required. At these time points, free GalNAlk-1-phosphate is clearly detectable (Fig. S3) These data indicated that WT-AGX1 is likely the rate-determining step in the biosynthesis of UDP-GalNAlk **1** and UDP-GlcNAlk **2**. Overexpression of mut-AGX1 likely renders the upstream activation steps NAGK/AGM and GALK2 rate-determining.

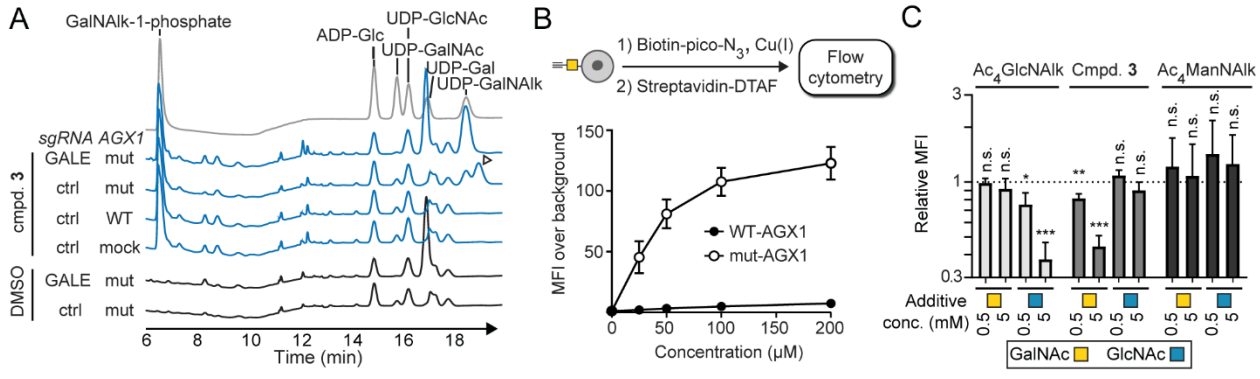

Fig. 2: mut-AGX1-mediated biosynthesis of UDP-GalNAlk **1** and cell surface labeling. *A*, metabolite profiling of K-562 cells based on AGX1 expression and presence of GALE by HPAEC. Grey trace represents standards. Arrowhead depicts epimerization of UDP-GalNAlk **1** to UDP-GlcNAlk **2**. Data are representative of two independent experiments. *B*, dose response of cell surface labeling of AGX1-stably transfected K-562 cells after feeding **3** as assessed by flow cytometry. Data are means ± SEM as fold increase from DMSO-treated cells from at least three independent experiments. Error bars for WT-AGX1 data are too small to be shown. *C*, competition of cell surface labeling in mut-AGX1-transfected GALE-KO K-562 cells fed with 50 μM caged GalNAlk-1-phosphate **3**, 50 μM Ac_4GlcNAlk or 10 μM Ac_4ManNAlk by different concentrations of GalNAc or GlcNAc. Data are from three independent experiments. Statistical significance was assessed by unpaired, two-tailed t test against labeling experiments without additives (dashed line). Asterisks indicate *P* values: **P* < 0.05; ***P* < 0.01; ****P* < 0.001; n.s. non-significant. DTAF = Dichlorotriazinylamino fluorescein; MFI = median fluorescence intensity.

We next visualized the impact of metabolic engineering on glycoprotein labeling by Ac_4GalNAlk and Ac_4GlcNAlk. Following feeding of AGX1-transfected K-562 cells with alkyne-containing monosaccharide precursors, cell surfaces were either treated with a neuraminidase or left untreated. The living cells were then subjected to CuAAC with the clickable near-infrared fluorophore CF680 picolyl azide, and labeled cell surface glycoproteins were analyzed by in-gel fluorescence.[17] Under these conditions, the compounds Ac_4GalNAlk, Ac_4GlcNAlk and caged GalNAlk-1-phosphate **3** exhibited mut-AGX1-dependent labeling while the control reagent Ac_4ManNAlk labeled glycoproteins irrespective of the AGX1 construct used (Fig. 3A). Treatment with a non-specific sialidase led to an increase of signal in all cases except for Ac_4ManNAlk-labeled cells, consistent with increased availability of GalNAc- and GlcNAc-carrying alkyne tags towards click reagents when the layer of sialic acid is enzymatically trimmed.[11,17] Of note, the dependence on mut-AGX1 for GalNAlk/GlcNAlk labeling emphasizes that

UDP-sugar formation is a prerequisite for efficient labeling, excluding previously reported non-enzymatic cysteine glycosylation that typically happens under very high concentrations of per-acetylated sugars.[22,23] We next visualized glycocalyx labeling by fluorescence microscopy on AGX1-transfected murine 4T1 cells. Clickable biotin picolyl azide and Streptavidin-AF647 readily detected a large enhancement of Ac_4GalNAlk-mediated cell surface labeling in cells stably expressing mut-AGX1 over non-transfected cells (Fig. 3B). In contrast, cell surface labeling by the AGX1-independent MOE reagent Ac_4ManNAlk was remained unchanged upon mut-AGX1 transfection (Fig. S4).

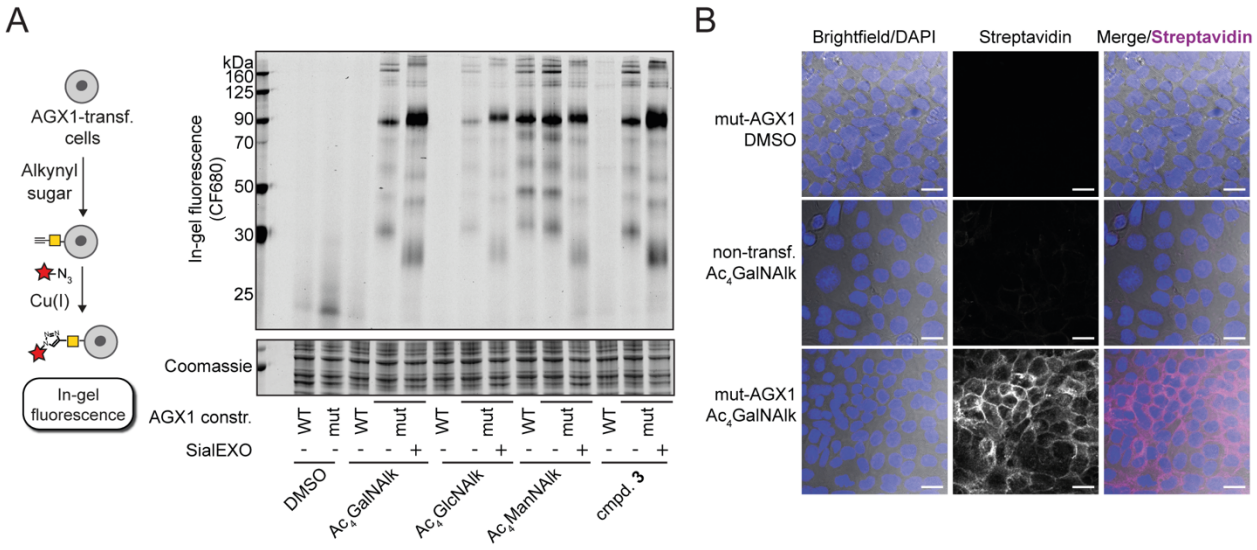

Fig. 3: mut-AGX1 enables efficient metabolic labeling with caged precursors of GalNAlk and GlcNAlk. *A*, cell surface labeling of AGX1-transfected K-562 cells fed with 50 µM Ac_4GalNAlk, 50 µM Ac_4GlcNAlk, 10 µM Ac_4ManNAlk or 25 µM caged GalNAlk-1-phosphate **3** as assessed by on-cell CuAAC with the NIR fluorophore CF680-picolyl azide and in-gel fluorescence. Data are representative of two independent experiments. *B*, fluorescence microscopy of mut-AGX1-expressing of non-transfected 4T1 cells fed with DMSO or 25 µM Ac_4GalNAlk, treated with biotin-picolyl-azide under on-cell CuAAC conditions and visualized with Streptavidin-AF647. Data are representative of two independent experiments. Scale bar, 20 µm.

Due to GALE-mediated interconversion of UDP-GalNAlk and UDP-GlcNAlk, the glycoprotein profile labeled by both MOE reagents Ac_4GalNAlk and Ac_4GlcNAlk is identical (Fig. 3A). To assess the contribution of each UDP-sugar to signal, we profiled the glycoprotein patters in GALE-KO cells that functionally separate UDP-GalNAlk **1** and UDP-GlcNAlk **2** (Fig 4A). Cells were grown in GalNAc-containing media to maintain native levels of metabolites such as UDP-GalNAc, allowing for comparison with GALE-expressing control cells when all cell lines were transfected with mut-AGX1. While GALE-expressing control cells displayed identical labeling patterns when fed with either Ac_4GalNAlk or Ac_4GlcNAlk, GALE-KO had a striking effect on labeling patterns. UDP-GalNAlk **1** contributed highly intense glycoprotein bands at approx. 100 kDa and 40 kDa, while UDP-GlcNAlk **2** contributed a diffuse pattern of lower overall intensity (Fig. 4A). We speculated that the intense bands labeled by UDP-GalNAlk **1** are highly GalNAc-glycosylated mucin domain-containing glycoproteins. To test this notion, we subjected GalNAlk-fed and CF680-picolyl azide labeled K-562 cells to different concentrations of the mucin protease StcE or the more promiscuous O-glycoprotease OpeRATOR (Fig. S5).[24] Treatment with both proteases led to a decrease of cell surface glycoprotein signal in a dose-dependent manner, while signal was recovered as fluorescently labeled broad bands of lower molecular weight in the supernatant. These data confirm that GalNAlk enters mucin domain-containing proteins and other O-GalNAc-glycosylated proteins. Further, we compared the Ac_4GlcNAlk and Ac_4GalNAlk labeling band patterns in GALE-KO or control cells with previously characterized, azide-containing MOE reagents Ac_4GlcNAz, Ac_4GalNAz. Both reagents are converted to azide-tagged UDP-GlcNAc/GalNAc analogs that are interconvertible by GALE.[10–12] We further used the O-GalNAc-specific reagent Ac_3GalNAzMe-1-P$(SATE)_2$ **4** that is a precursor to epimerization-resistant UDP-GalNAzMe that is not a substrate for GALE in the living cell (Fig 4B).[11] To ensure that band patterns are comparable between azide- and alkyne-tagged monosaccharides, we used the same NIR-fluorophore CF680 with either alkyne or picolyl azide groups for CuAAC. Ac_4GlcNAz/Ac_4GalNAz showed a similar pattern to Ac_4GlcNAlk/Ac_4GalNAlk

in labeling different glycoprotein subsets upon GALE-KO, although the number of glycoprotein bands was higher with azide-tagged monosaccharide analogs. These findings are in line with UDP-GalNAz being a better substrate for the commonly expressed GalNAc-T1 and T2 than UDP-GalNAlk **1** (Fig. 1C).[11,19] The Ac_4GalNAlk-labeled band pattern in GALE-KO cells resembled a subset of O-GalNAc glycoproteins labeled by **4**. Taken together, these data suggest that UDP-GalNAlk **1** and UDP-GlcNAlk **2** label different sets of glycoproteins but are interconnected by GALE in the living cell. Structurally simple azide- and alkyne-tagged GalNAc/GlcNAc derivatives label particular glycoprotein subsets and should thus serve as orthogonal, but potentially complementary MOE reagents in the presence of mut-AGX1.

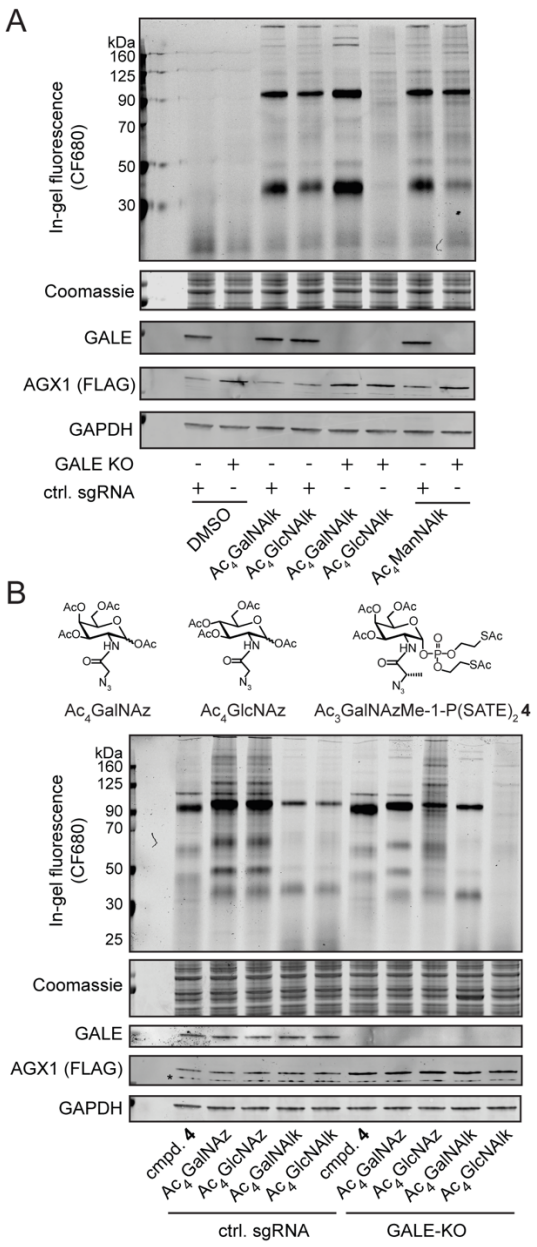

227

228 **Fig. 4:** GalNAlk and GlcNAlk-mediated labeling of glycoprotein subsets. *A*, cell surface labeling of mut-
229 AGX1-transfected K-562 GALE-KO or control sgRNA-expressing cells fed with 10 μM Ac_4GalNAlk, 50
230 μM Ac_4GlcNAlk, or 10 μM Ac_4ManNAlk as assessed by on-cell click chemistry and in-gel fluorescence.
231 Data are representative of two independent experiments. *B*, comparison of cell surface labeling of mut-
232 AGX1-transfected K-562 GALE-KO or control sgRNA-expressing cells fed with 10 μM Ac_4GalNAlk, 50

μM Ac_4GlcNAlk, 3 μM Ac_4GalNAz, 8 μM Ac_4GlcNAz or 100 μM caged GalNAzMe-1-phosphate **4**. Data are representative of two independent experiments.

We have shown that comprehensive metabolic profiling can turn weak MOE reagents into efficient chemical biology tools to profile cellular glycosylation. The expression of mut-AGX1 enhances labeling by Ac_4GalNAlk and Ac_4GlcNAlk by orders of magnitude, substantially expanding the toolbox for glycobiology. While our approach relies cell transfection, the plasmids we use are based on transposase-mediated stable integration which is compatible even with hard-to-transfect cell lines and more complex model systems such as organoids.[11]

Author contributions

A.C., M.F.D., J.T.B., C.R.B. and B.S. conceived the project and planned experiments; A.C., G.B.-T., A.J.A. H.L.D. and B.S. performed experiments; J.C., T.W., W.B., C.R. and S.K. made and contributed key reagents; A.C., G. B.-T., A.J.A., M.F.D. and B.S. analyzed data; A.C., G. B.-T. and B.S. wrote the paper with input from all authors.

Acknowledgements

We thank Douglas Fox for help with HPAEC experiments, Kayvon Pedram for providing StcE, Matthew R. Pratt for helpful discussions, Phil Walker for advice on vector choice, and Acely Garza-Garcia for helpful discussions on HPLC. We thank Rocco D'Antuono of the Crick Advanced Light Microscopy STP for support and assistance in this work. We are grateful for support by the Francis Crick Institute Cell Services and Peptide Chemistry Science Technology Platforms. We are thankful for generous funding by Stanford University, Stanford Chemistry, Engineering & Medicine for Human Health (ChEM-H) and Howard Hughes Medical Institute. This work was supported by NIH Grant R01 CA200423 (to C.R.B.), and by the Francis Crick Institute (A.C., G.B.-T. and B.S.), which receives its core funding from Cancer Research UK Grant FC001749, UK Medical Research Council Grant FC001749, and Wellcome Trust

Grant FC001749. M.F.D. was supported by a Dutch Research Council (NWO) Rubicon Postdoctoral Fellowship. W.M.B. was supported by a PhD studentship funded by Engineering and Physical Sciences Research Council (EPSRC) Centre for Doctoral Training in Chemical Biology – Innovation for the Life Sciences Grant EP/S023518/1 and GlaxoSmithKline. H.L.D. acknowledges funds from Wellcome Trust New Investigator Award 104785/B/14/Z. A.J.A. was supported by a Stanford ChEM-H undergraduate scholarship.

References

(1) Sletten, E. M.; Bertozzi, C. R. Bioorthogonal Chemistry: Fishing for Selectivity in a Sea of Functionality. *Angew. Chem. Int. Ed.* **2009**, *48* (38), 6974–6998. https://doi.org/10.1002/anie.200900942.

(2) Parker, C. G.; Pratt, M. R. Click Chemistry in Proteomic Investigations. *Cell*. Elsevier Inc. 2020, pp 605–632. https://doi.org/10.1016/j.cell.2020.01.025.

(3) Zol-Hanlon, M. I.; Schumann, B. Open Questions in Chemical Glycobiology. *Commun. Chem.* **2020**, *3* (1), 1–5. https://doi.org/10.1038/s42004-020-00337-6.

(4) Cioce, A.; Malaker, S. A.; Schumann, B. Generating Orthogonal Glycosyltransferase and Nucleotide Sugar Pairs as Next-Generation Glycobiology Tools. *Current Opinion in Chemical Biology*. Elsevier Ltd February 1, 2021, pp 66–78. https://doi.org/10.1016/j.cbpa.2020.09.001.

(5) Mahal, L. K.; Yarema, K. J.; Bertozzi, C. R. Engineering Chemical Reactivity on Cell Surfaces through Oligosaccharide Biosynthesis. *Science* **1997**, *276* (5315), 1125–1128. https://doi.org/10.1126/science.276.5315.1125.

(6) Hang, H. C.; Yu, C.; Pratt, M. R.; Bertozzi, C. R. Probing Glycosyltransferase Activities with the Staudinger Ligation. *J. Am. Chem. Soc.* **2004**, *126* (1), 6–7. https://doi.org/10.1021/ja037692m.

(7) Zaro, B. W.; Yang, Y. Y.; Hang, H. C.; Pratt, M. R. Chemical Reporters for Fluorescent Detection and Identification of O-GlcNAc-Modified Proteins Reveal Glycosylation of the Ubiquitin Ligase NEDD4-1. *Proc. Natl. Acad. Sci. U. S. A.* **2011**, *108* (20), 8146–8151. https://doi.org/10.1073/pnas.1102458108.

(8) Besanceney-Webler, C.; Jiang, H.; Zheng, T.; Feng, L.; Soriano Del Amo, D.; Wang, W.; Klivansky, L. M.; Marlow, F. L.; Liu, Y.; Wu, P. Increasing the Efficacy of Bioorthogonal Click Reactions for Bioconjugation: A Comparative Study. *Angew. Chem. Int. Ed.* **2011**, *50* (35), 8051–8056. https://doi.org/10.1002/anie.201101817.

(9) Peneff, C.; Ferrari, P.; Charrier, V.; Taburet, Y.; Monnier, C.; Zamboni, V.; Winter, J.; Harnois, M.; Fassy, F.; Bourne, Y. Crystal Structures of Two Human Pyrophosphorylase Isoforms in Complexes with UDPGlc(Gal)NAc: Role of the Alternatively Spliced Insert in the Enzyme Oligomeric Assembly and Active Site Architecture. *EMBO J.* **2001**, *20* (22), 6191–6202. https://doi.org/10.1093/emboj/20.22.6191.

(10) Boyce, M.; Carrico, I. S.; Ganguli, A. S.; Yu, S. H.; Hangauer, M. J.; Hubbard, S. C.; Kohler, J. J.; Bertozzi, C. R. Metabolic Cross-Talk Allows Labeling of O-Linked β-N- Acetylglucosamine-Modified Proteins via the N-Acetylgalactosamine Salvage Pathway. *Proc. Natl. Acad. Sci. U. S. A.* **2011**, *108* (8), 3141–3146. https://doi.org/10.1073/pnas.1010045108.

(11) Debets, M. F.; Tastan, O. Y.; Wisnovsky, S. P.; Malaker, S. A.; Angelis, N.; Moeckl, L. K. R.; Choi, J.; Flynn, H.; Wagner, L. J. S.; Bineva-Todd, G.; Antonopoulos, A.; Cioce, A.; Browne, W. M.; Li, Z.; Briggs, D. C.; Douglas, H. L.; Hess, G. T.; Agbay, A. J.; Roustan, C.; Kjaer, S.; Haslam, S. M.; Snijders, A. P.; Bassik, M. C.; Moerner, W. E.; Li, V. S. W.; Bertozzi, C. R.; Schumann, B. Metabolic Precision Labeling Enables Selective Probing of O-Linked N -Acetylgalactosamine Glycosylation . *Proc. Natl. Acad. Sci. U. S. A.* **2020**, *117* (41), 25293–25301. https://doi.org/10.1073/pnas.2007297117.

(12) Shajahan, A.; Supekar, N. T.; Wu, H.; Wands, A. M.; Bhat, G.; Kalimurthy, A.; Matsubara, M.; Ranzinger, R.; Kohler, J. J.; Azadi, P. Mass Spectrometric Method for the Unambiguous Profiling of Cellular Dynamic Glycosylation. *ACS Chem. Biol.* **2020**, *15* (10), 2692–2701. https://doi.org/10.1021/acschembio.0c00453.

(13) Hang, H. C.; Yu, C.; Kato, D. L.; Bertozzi, C. R. A Metabolic Labeling Approach toward Proteomic Analysis of Mucin-Type O-Linked Glycosylation. *Proc. Natl. Acad. Sci. U. S. A.* **2003**, *100* (25), 14846–14851. https://doi.org/10.1073/pnas.2335201100.

(14) Woo, C. M.; Iavarone, A. T.; Spiciarich, D. R.; Palaniappan, K. K.; Bertozzi, C. R. Isotope-Targeted Glycoproteomics (IsoTaG): A Mass-Independent Platform for Intact N- and O-Glycopeptide Discovery and Analysis. *Nat. Methods* **2015**, *12* (6), 561–567. https://doi.org/10.1038/nmeth.3366.

(15) Pouilly, S.; Bourgeaux, V.; Piller, F.; Piller, V. Evaluation of Analogues of GalNAc as Substrates for Enzymes of the Mammalian GalNAc Salvage Pathway. *ACS Chem. Biol.* **2012**, *7* (4), 753–760. https://doi.org/10.1021/cb200511t.

(16) Yu, S. H.; Boyce, M.; Wands, A. M.; Bond, M. R.; Bertozzi, C. R.; Kohler, J. J. Metabolic Labeling Enables Selective Photocrosslinking of O-GlcNAc-Modified Proteins to Their Binding Partners. *Proc. Natl. Acad. Sci. U. S. A.* **2012**, *109* (13), 4834–4839. https://doi.org/10.1073/pnas.1114356109.

(17) Schumann, B.; Malaker, S. A.; Wisnovsky, S. P.; Debets, M. F.; Agbay, A. J.; Fernandez, D.; Wagner, L. J. S.; Lin, L.; Li, Z.; Choi, J.; Fox, D. M.; Peh, J.; Gray, M. A.; Pedram, K.; Kohler, J. J.; Mrksich, M.; Bertozzi, C. R. Bump-and-Hole Engineering Identifies Specific Substrates of Glycosyltransferases in Living Cells. *Mol. Cell* **2020**, *78*, 1–11. https://doi.org/10.1016/j.molcel.2020.03.030.

(18) Batt, A. R.; Zaro, B. W.; Navarro, M. X.; Pratt, M. R. Metabolic Chemical Reporters of Glycans

Exhibit Cell-Type-Selective Metabolism and Glycoprotein Labeling. *ChemBioChem* **2017**, *18* (13), 1177–1182. https://doi.org/10.1002/cbic.201700020.

(19) Choi, J.; Wagner, L. J. S.; Timmermans, S. B. P. E.; Malaker, S. A.; Schumann, B.; Gray, M. A.; Debets, M. F.; Takashima, M.; Gehring, J.; Bertozzi, C. R. Engineering Orthogonal Polypeptide GalNAc-Transferase and UDP-Sugar Pairs. *J. Am. Chem. Soc.* **2019**, *141* (34), 13442–13453. https://doi.org/10.1021/jacs.9b04695.

(20) de las Rivas, M.; Lira-Navarrete, E.; Gerken, T. A.; Hurtado-Guerrero, R. Polypeptide GalNAc-Ts: From Redundancy to Specificity. *Current Opinion in Structural Biology*. Elsevier Ltd 2019, pp 87–96. https://doi.org/10.1016/j.sbi.2018.12.007.

(21) Uttamapinant, C.; Tangpeerachaikul, A.; Grecian, S.; Clarke, S.; Singh, U.; Slade, P.; Gee, K. R.; Ting, A. Y. Fast, Cell-Compatible Click Chemistry with Copper-Chelating Azides for Biomolecular Labeling. *Angew. Chem. Int. Ed.* **2012**, *51* (24), 5852–5856. https://doi.org/10.1002/anie.201108181.

(22) Qin, W.; Qin, K.; Fan, X.; Peng, L.; Hong, W.; Zhu, Y.; Lv, P.; Du, Y.; Huang, R.; Han, M.; Cheng, B.; Liu, Y.; Zhou, W.; Wang, C.; Chen, X. Artificial Cysteine S-Glycosylation Induced by Per-O-Acetylated Unnatural Monosaccharides during Metabolic Glycan Labeling. *Angew. Chem. Int. Ed.* **2018**, *57* (7), 1817–1820. https://doi.org/10.1002/anie.201711710.

(23) Qin, K.; Zhang, H.; Zhao, Z.; Chen, X. Protein S-Glyco-Modification through an Elimination-Addition Mechanism. *J. Am. Chem. Soc.* **2020**, *142* (20), 9382–9388. https://doi.org/10.1021/jacs.0c02110.

(24) Malaker, S. A.; Pedram, K.; Ferracane, M. J.; Bensing, B. A.; Krishnan, V.; Pett, C.; Yu, J.; Woods, E. C.; Kramer, J. R.; Westerlind, U.; Dorigo, O.; Bertozzi, C. R. The Mucin-Selective Protease StcE Enables Molecular and Functional Analysis of Human Cancer-Associated Mucins. *Proc. Natl. Acad. Sci. U. S. A.* **2019**, *116* (15), 7278–7287.

https://doi.org/10.1073/pnas.1813020116.